Calculation of Spectral Degradation due to Contaminant Films on Infrared and Optical Sensors

Lara Gamble[*a], J.R. Dennison[b], Bobby Wood[c], James Herrick[a], and James S. Dyer[a]
[a]Space Dynamics Laboratory, USU; [b]Dept. of Physics, USU; [c]Bob Wood Aerospace Consulting Services, Inc. (BWACS) Tullahoma, TN

ABSTRACT

Molecular surface contaminants can cause degradation of optical systems, especially if the contaminants exhibit strong absorption bands in the region of interest. Different strategies for estimation of spectral degradation responses due to uniform films for various types of systems are reviewed. One tool for calculating the effects of contaminant film thickness on signal degradation in the mid IR region is the simulation program CALCRT. The CALCRT database will be reviewed to correlate spectral n and k values associated with specific classes of organic functional groups. Various schemes are also investigated to estimate the spectral degradation in the UV-Vis region. Experimental measurements of reflectance changes in the IR to UV-Vis regions due to specific contaminants will be compared. Approaches for estimating changes in thermal emissivity and solar absorptivity will also be discussed.

Keywords: Optical constants, cryogenic, contamination, infrared, emissivity

1. INTRODUCTION

The build up of molecular film contaminants on cold optics or detectors can affect the function of a spectrometer. One of the most common molecular film contaminants in cryogenic applications is water-ice. Water can have an appreciable vapor pressure in the spectrometer due to the outgassing of multilayer insulation (MLI) blanketing, as well as other materials, around the spectrometer. Other contaminants or mixture of molecular contaminants may also be introduced into the system by the presence of paints, composites, and other materials found in the spectrometer chamber. These contaminants may include CO_2, silicone, or generic hydrocarbon that can also affect signal intensity for specific bandpass regions. Contaminants can be a great problem to the optimal operation of infrared and optical systems. This problem has been the subject of various investigations, with only a few examples sited here[1-5].

Infrared (IR) radiation in the ~10,000-100 cm^{-1} range is absorbed by molecules and converted into molecular vibrations[6]. For example, the strongest absorption for water-ice is seen at ~3300 cm^{-1} (or ~3 μm) which is due to excitation of the OH bond stretch. The amount of energy absorbed by the molecular films is directly related to the overall decrease in the amount of light that reaches a detector. The amount of light that is lost is also proportional to the thickness of the film (or amount of molecules present). The simplest example of this is found in Beer's law:

$$I/I_0 = e^{-\varepsilon bc} \qquad \text{Eqn. 1}$$

Where 'I' is the detected intensity 'I_0' is original intensity, 'ε' is a molar absorbtivity (absorption coefficient) and 'b' is the thickness of the sample, and 'c' is the concentration (or density) of the sample. Similarly, the amount of signal lost in a cold IR spectrometer can be related to the amount of contaminant film on the optics.

Calculations can be used to predict the effects of contaminant films on IR spectrometers and may also be used to determine what type of contamination is causing degradation in a spectrometer. Similar types of calculations have been

[*] lara.gamble@sdl.usu.edu; phone: (435)797-4686; fax: (435)797-4366; Space Dynamics Laboratory, 1695 North Research Parkway, North Logan, Utah, 84341

Optical System Contamination: Effects, Measurements, and Control VII, Philip T. Chen
O. Manuel Uy, Editors, Proceedings of SPIE Vol. 4774 (2002) © 2002 SPIE · 0277-786X/02/$15.00

discussed before in other papers[4,5]. A computer program that calculates the optical properties of films of various thicknesses is CALCRT[1,2], a Fortran program which uses n and k values to determine reflectance and transmittance spectra for contaminant films on optical surfaces. This program has been a useful tool not only to determine acceptable contaminant levels for contaminantion control plans, but has also been used to identify the cause for signal loss. These program has been useful for IR instruments at SDL including SABER (Sounding of the Atmosphere using Broadband Emission Spectroscopy)[7]and others.

In this paper, the applications of the CALCRT tool will be investigated for identifying absorption bands of common contaminants, calculating the effect of a contaminant film in a specified bandpass region, and discussing the possibility for using this program to determine effects outside of the IR region. The potential for the CALCRT tool to predict changes in emissivity due to contaminant films will also be discussed.

2. RESULTS/ DISCUSSION

2.1 Background on CALCRT

The program CALCRT [1-3] (CALCulations of Reflectance and Transmittance) is a Fortran program that calculates the spectral transmittance and reflectance of a thin film on a specified substrate in two different manners: 1) as a function of wavelength for a specified thickness of "contaminant" film, or 2) as a function of film thickness for a specified incoming wavelength. Multiple internal reflections are considered. This program assumes a uniform film on the surface, no BRDF effects are considered.

The optical constants of the film (n and k values as a function of wavenumber) must be supplied to the program, as well as the optical constants for substrates not calculated by the program. Other data that must be supplied are the thickness of the substrate, film, and the incident angle of the beam. By using the optical constants (n and k values) as well as allowing for different incident beam angles, CALCRT calculates individual results for both types of polarization (**s** and **p**). This feature is useful to determine how thin film contaminants will affect incident polarized beams. While CALCRT is capable of calculating reflectance and transmittance spectra at various incident beam angles, unless otherwise noted the incident angle of the beam in calculations used in this paper was 0° (or normal incidence). At normal incidence there is not distinction between **s** and **p** polarized light.

A "library" of n and k values are supplied with the CALCRT program. The n and k values for the CALCRT "library" were obtained experimentally from contaminants of real outgassing products as well as common gaseous contaminants such as water or CO_2 (for example in References 1-3,8). Materials were heated to ~125°C and the outgassing products condensed on the test sample to obtain the n and k values. The library states what material is outgassing to identify the n and k values (for example RTV-560). It should be remembered that the supplied optical constants are for the contaminants produced from the outgassing of the specified material and do not necessarily represent the material itself. However, a reflectance spectrum generated from the n and k values can be used to identify what types of molecules the n and k data represent (such as generic hydrocarbon or ether linkages). It should be noted that additional n and k values were obtained from other sources[9,10,11] and used in the CALCRT program to expand the results to different substrates and wavenumber regions than those available in the CALCRT n and k library. These results are discussed in the following section.

An example of the CALCRT output (reflection as a function of wavenumber) is shown in Figure 1 for a 1000nm film of CO_2 on a gold substrate. A bare gold substrate reflectance output is shown for comparison. (Note: Gold substrate is opaque and CALCRT simulations accordingly showed zero transmittance of the incoming beam.) The n & k values for the film were determined experimentally[8] for the mid IR region of ~700-4000 cm^{-1} (~3-14μm wavelength). The gold n and k values were derived from Palik[9].

A decrease in reflectance is seen as absorption peaks specific to CO_2. These peaks are due to the absorption of the beam at wavelengths that correspond to the molecular vibrational frequencies of CO_2. As can be seen in Figure 1, a 1000nm CO_2 film only absorbs appreciably at ~2340 cm^{-1} (due to the O=C=O stretching frequencies). An increase in these absorption peaks (corresponding to a decrease in the reflected signal) is seen at these specific wavelengths as the amount of CO_2 film is increased on the surface.

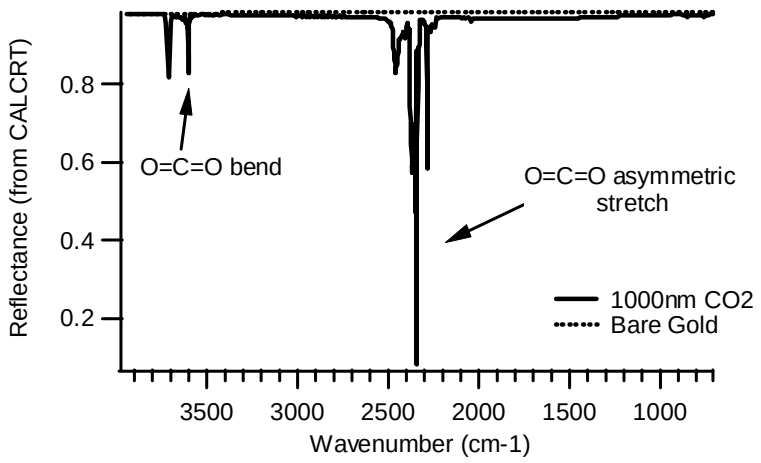

Figure 1: CALCRT calculated reflectance spectra from bare gold surface and a gold substrate with 1000nm CO_2 film.

2.2 Calculated degradation of signal intensity due to contaminant films

When appropriate n and k values for a desired film and substrate are chosen, CALCRT generated spectra can be used to calculate expected degradation of the signal due to the presence of the contaminant. The "Signal Performance" of a surface (or mirror) is defined here as the ratio of the degraded signal response to the optimum signal response. The signal response is determined by integrating a combination of the reflectance (which is generated by CALCRT), the relative spectral response (RSR) curve for the spectrometer, and a blackbody curve for the temperature of interest. For the degraded signal the reflectance would be reflectance of the surface plus the contaminant film. For the "control" or optimum signal response a reflectance spectrum of the uncontaminated substrate is used. This is demonstrated below in Equation 2 for assuming the reflecting substrate is a gold.

$$"SignalPerformance" = \frac{\int R_{Au+film}(\lambda) \cdot RSR(\lambda) \cdot BB_T(\lambda) d\lambda}{\int R_{BareAu}(\lambda) \cdot RSR(\lambda) \cdot BB_T(\lambda) d\lambda} \qquad \text{Eqn. 2}$$

$R_{au+film}$ = CALCRT Calculated Reflectance from water film on gold
$R_{Bare\ Au}$ = CALCRT Calculated Reflectance from bare gold
RSR = Relative spectral response (experimentally measured for DXPS)
BB_T = Blackbody emission spectrum at temperature T (°K)

The range of the bandpass region (related to the RSR) can determine to what degree a contaminant film affects a signal. Figure 2 shows the CALCRT calculated reflectance for a 1000 nm film of water-ice on a gold substrate (the substrate is assumed to be at ~80 K). The heavy and dotted lines show the average signal performance for two different bandpass regions with the 1000 nm of water-ice on the gold substrate. These results were calculated using Equation 2 with 300 K blackbody and a square wave over the region of interest for the RSR.

The average signal performance for a bandpass region limited to the range of 3100-3400 cm^{-1} (heavy line in Figure 2) reduced to ~0.1 (or 10% of the original signal performance) when 1000 nm of ice is absorbed on the substrate. It is obvious that this region will be greatly affected by an adsorbed film of ice because it directly overlaps a large portion of the ~3300 cm^{-1} absorption band for the –OH stretch. In contrast the larger bandpass region of 2100-3400 cm^{-1} still has an average signal performance of ~0.85 (or 85% of the original signal). While this region still overlaps the large absorption peak due to the OH stretch, the region does not see as much degradation since the affects of the -OH absorption band are reduced due to the contribution of regions that do not see as much absorption. As a direct result of

these calculations, it is obvious that a spectrometer with a smaller bandpass region which is directly over an absorption band will have to have much more stringent contamination control requirements than one with a broader bandpass region.

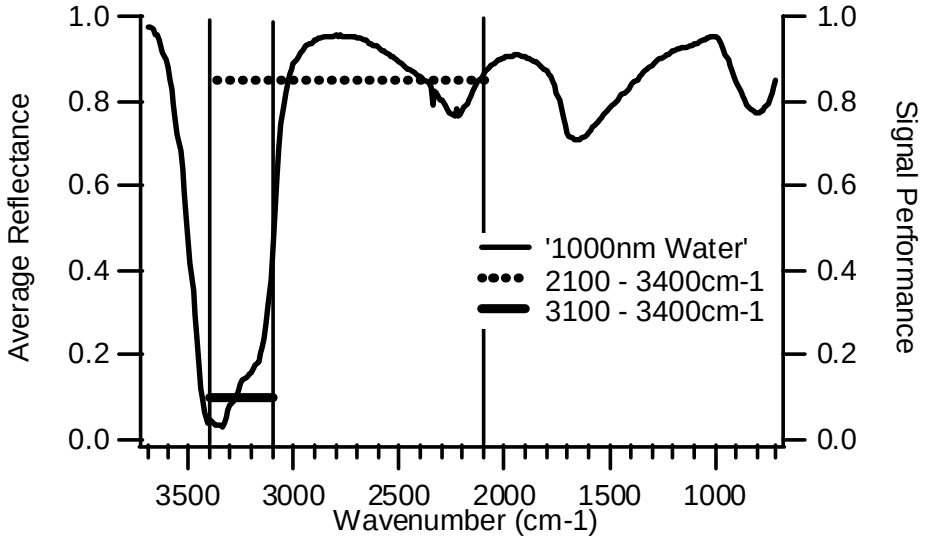

Figure 2: CALCRT calculated reflectance for 1000nm water on gold and the signal performance for a bandpass region of 2100-3400 cm^{-1} compared to 3100-3400cm-1.

The signal performance of specific bandpass regions can also be followed as a function of film thickness as shown in Figure 3. This type of graph is a useful reference when creating a contamination budget for a spectrometer. The degradation in signal can be followed and compared for each bandpass region used by a spectrometer and the contamination budget can be designed to accommodate the most sensitive region. Figure 3 followed the two regions shown above in Figure 2 as a function of film thickness.

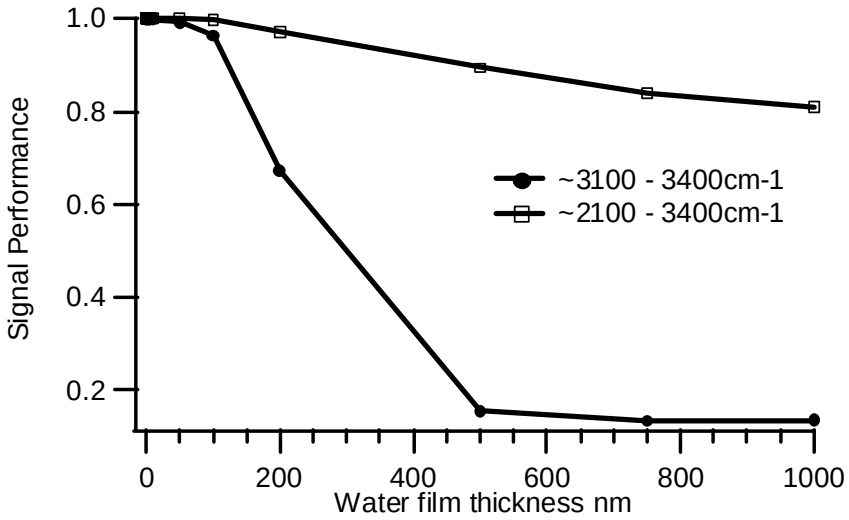

Figure 3: The signal performance as a function of increasing water-ice thickness for the 3100-3400 cm^{-1} and the 2100-3400 cm^{-1} regions.

Again, each point on the curve was calculated using Equation 2 and a 300 K blackbody. At 20 nm of water-ice contamination there is little degradation in either region, but by 100 nm there is ~5% loss in the 3100-3400 cm^{-1} region signal. After 100 nm this signal begins to drop dramatically. By 1000 nm the signal performances is reduced to 10% of for the 3100-3400 cm^{-1} region and 85% for the 2100-3400 cm^{-1} region.

It should be noted that these calculations are only assuming one reflecting surface. Actual spectrometers will contain more than one mirror surface as well as beam splitters, windows, and a detector. These other surface must be considered in combination when developing a contamination budget.

2.3 Applications to the Visible and UV regions

In theory, the CALCRT calculations can be applied to other regions of the electro-magnetic spectrum as long as accurate n and k values can be found. Species such as H_2O-ice hold an interest for many different groups, and "expanded" regions of n and k values are available[11]. However, previous papers have discussed the importance of accurate n and k values and discussed how deviation of theoretical results from experimental ones may be due to this inaccuracy[4]. Consequently, the CALCRT results using the "expanded region" of n and k values for H_2O-ice from Warren et al. in Reference 11 are compared to the result was using the CALCRT supplied n and k values for H_2O-ice. This comparison is shown in Figure 4 for a 1000 nm H_2O-ice film on a gold substrate.

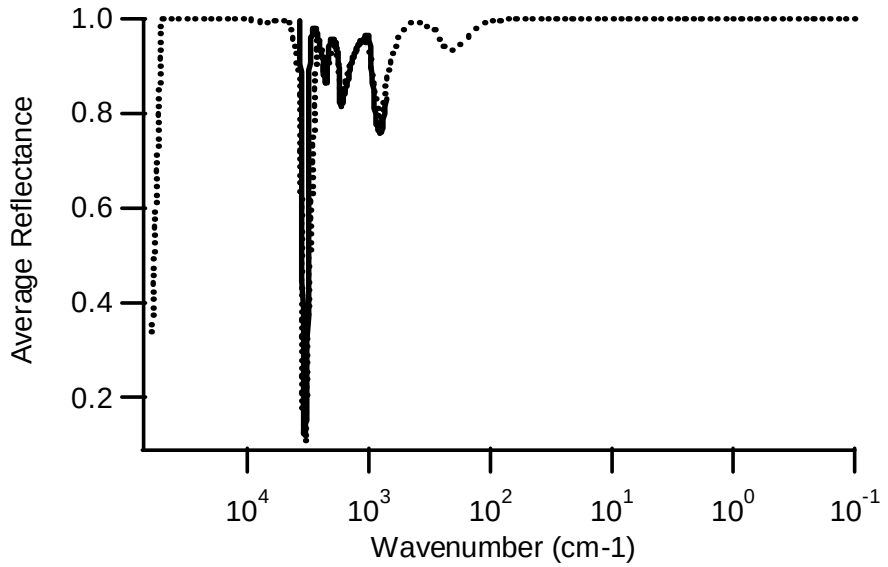

Figure 4: will be the absorption spectrum of 1000 nm water on gold substrate using CALCRT n and k values (solid line) and n and k values from Warren et al. in Ref. 11 (dashed line).

The n and k values for the gold substrate was derived from two different references[9,10]. As can be seen in Figure 4, there is fairly good agreement between the reflectance spectra calculated from the two different n and k sets. While the "expanded" n and k values do not have the resolution of the CALCRT values, it can be seen that the results still follow the same trend and correlate well within the mid-IR region. From this calculation it can be concluded that a 1000 nm film of water is not predicted to have an appreciable absorption in the visible-ultraviolet region of ~12500-50000 cm^{-1} (0.01 to 0.8 μm), excluding the Far-UV region, which could be a useful result for spectrometers that are investigating the Visible-UV region. This data indicates interesting potential for application of this type of calculations to the visible, UV, and other regions to determine contaminant effects on spectrometers. Other sources of contaminant n and k data have been identified and further investigation to the applications in the Visible-UV region are underway.

2.4 Calculated Changes in Emissivity

It has been known that contaminant films can affect the emissivity of a surface. A change in emissivity of an optic or thermal control surface that is kept cold by spacecraft cryo-coolers may result in an excessive heat load on the coolers. It would be helpful to be able to calculate the effects of contaminant films on thermal performance. Spectral hemispherical emittance can be determined from spectral hemispherical reflectance as shown below in Equation 3 (Kirchhoff's law):

$$\varepsilon_h = 1 - R_h \qquad \text{Eqn. 3}$$

Where ε_h is spectral emittance and R_h is spectral hemispherical reflectance. However, CALCRT calculates directional reflectance not hemispherical reflectance. To determine the spectral hemispherical reflectance, reflectance spectra were calculated at incident angles from 0° (normal incidence) to 80° (near glancing incidence) at 10° intervals. (The **s** and **p** polarized results are averaged to give the "unpolarized" result.) The spectral hemispherical emittance is then found by integrating at a specific wavelength over all of the angles[12,13] as shown in Equation 4.

$$\varepsilon_h(\lambda) = 1 - 2\int_0^{\pi/2} R_D(\theta,\lambda)\cos\theta\sin\theta d\theta \qquad \text{Eqn. 4}$$

In Equation 4 the incident angle of the beam is θ, and R_D is the directional reflectance (supplied by the CALCRT program). This calculation assumes that the reflectance is independent of the azimuthal angle ϕ, which is a reasonable assumption when assuming a flat, specular homogeneous substrate and film. Equation 4 produces a series of spectra as a function of wavelength at each incident angle.

While the spectral emittance is an interesting result, the total hemispherical emissivity is required for calculating changes in heat load on cryo-coolers. Total hemispherical emissivity is the ratio of the emissive power of the substrate in question to the emissive power of an ideal blackbody at the same temperature.

$$\varepsilon_T = \frac{\int P(\lambda,T)\varepsilon_h(\lambda)}{\int P(\lambda,T)} \qquad \text{Eqn. 5}$$

Where $P(\lambda,T)$ is the Planck's Function for a given wavelength and temperature. Once the spectral hemispherical emissivity is calculated (Equation 4), it can be inserted into Equation 5 at the appropriate blackbody temperature to give the total hemispherical emissivity.

Preliminary data has been calculated for water-ice film on a gold substrate using a 220 K blackbody. The thickness of the ice film was varied from bare gold substrate (no water) to 1000nm of H_2O-ice. Results of these calculations are shown in Figure 5. Each data point in Figure 5 represents the reflectance spectra for a specific thickness of H_2O -ice film integrated over all angles (Equation 4) followed by integration over all wavelengths (Equation 5).

One critical point to note with emissivity calculations is what temperature of blackbody was used for the calculations. The data shown in Figure 5 was calculated for a 220 K blackbody. The maximum intensity of a 220 K blackbody curve is at ~760 cm^{-1}. In Figure 5 the solid squares represent data calculated with the CALCRT limited range of n and k data (700-4000 cm^{-1}), which means that a good portion of the blackbody intensity is outside the range of this calculation. The open squares, however, are data calculated with a broader region (~0.2 to 100000cm-1), which covers the entire range of the blackbody intensity.

The emissivities calculated with these two different ranges of n and k values are slightly different, as can be seen in Figure 5. This difference is attributed to the fact that the n and k values limited to the 700-4000 cm^{-1} range do not account for the entire blackbody curve, as mentioned above, and therefore do not accurately calculate the emissivity of this ideal system. The broader region n and k values show the lower emissivity expected for an ideal surface. This conclusion is most easily demonstrated by a comparison of the emissivities calculated for bare gold using the two different n and k regions.

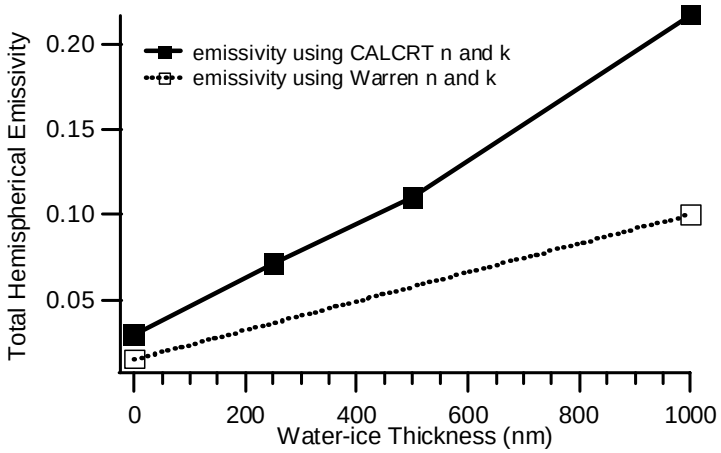

Figure 5: Total hemispherical emissivity calculations (Eqn. 5) for various thickness of water film on gold assuming a 220 K blackbody. The solid squares are results using CALCRT n and k values while the open squares are for larger wavenumber n and k values (Warren et al. in Ref 11).

The calculated emissivity for the bare gold substrate with a 220 K blackbody and using the CALCRT n and k values was 0.029. In contrast, the emissivity calculated with the longer range of n and k values[10] for the bare gold substrate was 0.015. While the emissivity of gold is often reported to be 0.02, it should be remembered that the experiment is limited by the "flatness" or specularity of the gold substrate. For example, the emissivity of vapor deposited gold is reported to be 0.031+/- 0.002 at 224 K[14]. In comparison, the emissivity determined experimentally for electro-deposited gold is reported to be much higher (0.038 at 197 K)[14]. The increased emissivity of the electro-deposited gold is due to the added scattering factor of the relatively "rougher" electrodeposited substrate versus a vapor deposited substrate. It is likely that the emissivity calculated here using the longer range n and k values is lower than experimental values because it is calculating a more "ideal" surface than cannot be easily be made.

A film of ice on a surface increases the emissivity of that surface (Figure 5). A relatively large amount (250μm) of ice on the surface is calculated to increase the emissivity of that surface to 0.936 (not shown), which is approaching the reported emissivity of smooth ice at 0.97. The two extremes of the emissivity calculations, gold with no ice film and gold with a large (250μm) ice film, are very close to their reported experimental values. The conclusion can be made that these emissivity calculations for a thin film of ice of the gold substrate is a good estimate of the actual change in emissivity that might be seen in a real spectrometer due to ice contaminant.

As previously mentioned, an increased emissivity of surfaces in cryo-systems should result in a greater heat load on the cryo-coolers. Further analyses are still under investigation to adequately interpret this data and determine if the theoretical results can be verified by the experimental observations. Modeled emissivities can be a useful tool for predicting changes is emissivity due to contaminant films, even though the calculations may not be accurate when calculating exact emissivities of "real life" surfaces.

3. CONCLUSIONS

The spectral degradation due to contaminant films can be determined using simple specular reflectance calculations. Care must be taken that the proper blackbody temperature and relative spectral response of the spectrometer are considered as well. Also, the calculations are dependant on the accuracy of the optical constants that are used. A limitation to usefulness of these calculations is the availability of accurate n and k values for contaminants of interest. Applications to the visible and UV regions are limited by the availability of optical constants in those regions as well. The CALCRT simulations may be applicable to calculating changes is emissivity. Data is promising and the general trend of the results is accurate, but more comparisons to experimental results still needs to be achieved to verify the precision of the calculations.

ACKNOWLEDGMENTS

The author would like to gratefully acknowledge Andrew Shumway for helpful discussions and references pertaining to emissivity calculations.

REFERENCES

1. B. E. Wood, W. T. Bertrand, R. J. Bryson, B. L. Seiber, P. M. Balco, R. A. Cull, "Surface Effects of Satellite Material Outgassing Products," *Journal of Thermophysics and Heat Transfer*, **2** (4), pp. 289-295, 1988.
2. B. E. Wood, W. T. Bertrand, E. L. Keich, Capt. J. D. Holt, and Capt. P. M. Falco, "Surface Effects of Satellite Materiall Outgassing Products," *AEDC-TR-89-2*, June 1989.
3. B. E. Wood and J. A Roux, "Infrared optical properties of thin H2O, NH3, and CO2 cryofilms," *J. Optical. Soc. America*, **72**, pp. 720-727, 1982.
4. Stephen V. Pepper, "Absorption of Infrared Radiation by Ice Cryodeposits," *NASA TN D-5181*, April 1969.
5. David D. Lynch and Ray W. Russell, "The detection of cryogenic water ice contaminants and the IR AI&T environment," *Proceedings of the SPIE*, **4130**, pp. 108-118, 2000.
6. R. Silverstien, G. Bassler, and T. Morril, *Spectrometric Identification of Organic Compounds (Forth Edition)*, John Wiley & Sons, 1981.
7. James Dyer et al, "Contamination Control of the SABAR Cryogenic Infrared Telescope," SPIE this conference , 2002.
8. J. Roux, B. Wood, and A. Smith "IR Optical Properties of Thin H_2O, NH_3, and CO_2 Croyfilms," *AEDC-TR-79-57*, September 1979.
9. E. Palik, *Handbook of Optical Constants of Solids*, pp294, 1985.
10. D. Lide, *CRC Handbook of Chemistry and Physics*, 72nd edition, 1991.
11. Th.Henning et al., "WWW database of optical constants for Astronomy," *Astron. Astrophys. Suppl.* **136**, p. 405, 1999.
12. Fred E. Nicodemus, "Directional Reflectance and Emissivity of and Opaque Surface," *Applied Optics*, **4**, pp767-773, 1965.
13. Andrew Shumway, "SPIRIT III Ground Calibration Equipment Characterization Report, Volume 2: Attachments," *SDL/94-073*, 1995.
14. J. G. Androulakis and L. H. Hemmerdinger, "Emissivity Measurement," *Contract NAS 5-21760*, November 1972.